

## An orbital floating time scale of the Hauterivian/Barremian GSSP from a magnetic susceptibility signal (Río Argos, Spain)

Mathieu Martinez<sup>a,\*</sup>, Pierre Pellenard<sup>a</sup>, Jean-François Deconinck<sup>a</sup>, Fabrice Monna<sup>b</sup>, Laurent Riquier<sup>c</sup>, Slah Boulila<sup>c</sup>, Mathieu Moiroud<sup>a</sup>, Miguel Company<sup>d</sup>

<sup>a</sup>UMR CNRS 6282 Biogéosciences, Université de Bourgogne, 6 bd Gabriel, F-21000 Dijon, France

<sup>b</sup>UMR CNRS 5594 ARTÉHIS, Université de Bourgogne, 6 bd Gabriel, F-21000 Dijon, France

<sup>c</sup>UMR CNRS 7193 ISTEP, UPMC Université Paris 06, cc 117, 4 pl. Jussieu, F-75252 Paris Cedex 05, France

<sup>d</sup>Departamento de Estratigrafía y paleontología, Facultad de Ciencias de Granada, 18002 Granada, Spain

### ARTICLE INFO

#### Article history:

Received 10 October 2011

Accepted in revised form 28 February 2012

Available online 22 March 2012

#### Keywords:

Hauterivian

Barremian

Faraoni

Cyclostratigraphy

Geologic Time Scale

### ABSTRACT

An orbital floating time scale of the Hauterivian–Barremian transition (Early Cretaceous) is proposed using high-resolution magnetic susceptibility measurements. Orbital tuning was performed on the Río Argos section (southeast Spain), the candidate for a Global boundary Stratotype Section and Point (GSSP) for the Hauterivian–Barremian transition. Spectral analyses of MS variations, coupled with the frequency ratio method, allow the recognition of precession, obliquity and eccentricity frequency bands. Orbitally-tuned magnetic susceptibility provides minimum durations for ammonite biozones. The durations of well-constrained ammonite zones are assessed at 0.78 myr for *Pseudothurmannia ohmi* (Late Hauterivian) and 0.57 myr for *Taveraidiscus hugii* (Early Barremian). These results are consistent with previous estimates from the other reference section (Angles, southeast France) and tend to show that the Río Argos section displays a complete succession for this time interval. They differ significantly from those proposed in the Geologic Time Scale 2008 and may help to improve the next compilation. The Faraoni Oceanic Anoxic Event, a key Early Cretaceous oceanographic perturbation occurring at the *P. ohmi*/*P. catulloi* subzone boundary has a duration estimated at 0.10–0.15 myr, which is similar to previous assessments.

© 2012 Elsevier Ltd. All rights reserved.

### 1. Introduction

Detailed biostratigraphy and sequence stratigraphy, correlated throughout Western Europe, provide a reference framework for studying the Late Hauterivian–Early Barremian stratigraphic interval (Hoedemaeker and Leereveld, 1995; Company et al., 2003; Hoedemaeker and Hergreen, 2003). However, the durations of the Hauterivian and Barremian stages are still being debated because (1) stage duration is based on a magnetostratigraphic model which postulates a constant rate for Hawaiian sea-floor spreading (Ogg and Smith, 2004) and (2) biozone and magnetochron intercalibration has recently been modified (McArthur et al., 2007). For instance, a duration of 1.9 myr was attributed to the latest Hauterivian *P. ohmi* Biozone in the Geologic Time Scale 2004 (GTS 2004; Gradstein et al., 2004), whereas a duration of only 0.2 myr was proposed for the same zone in the Geologic Time Scale 2008

(GTS 2008; Ogg et al., 2008). A cyclostratigraphic approach could provide independent data to constrain the duration of ammonite biozones and thus improve the next GTS (Hinnov and Ogg, 2007).

Earth's orbital cycles are known to have a strong periodic influence on climate and sedimentation (Hays et al., 1976). Palaeoclimate proxies are frequently used to detect orbital forcing in sedimentary series in order to establish accurate orbital time scales, notably for the Cenozoic (Lourens et al., 2004). Orbital forcing is also perceived in Cretaceous series, where numerous recent studies using cyclostratigraphic approaches have successfully extended the GTS up to that period (Locklair and Sageman, 2008; Voigt and Schönfeld, 2010; Husson et al., 2011). Magnetic susceptibility (MS) is a powerful proxy to detect palaeoclimate changes (Reynolds and King, 1995; Ellwood et al., 2000). It quantifies the ability of a sample to be magnetized in response to an external magnetic field. This response depends on the ferromagnetic, paramagnetic and diamagnetic mineral content of the sample. In hemipelagic environments, MS fluctuations are often inversely correlated to calcium carbonate content because this diamagnetic mineral, which is dominant in hemipelagic sediments, dilutes iron-bearing

\* Corresponding author. Tel.: +33 3 80 39 63 64.

E-mail address: [mathieu.martinez@u-bourgogne.fr](mailto:mathieu.martinez@u-bourgogne.fr) (M. Martinez).

minerals (Mayer and Appel, 1999; Weedon et al., 2004; Boullia et al., 2008). As a result, MS fluctuations largely reflect terrigenous flux and/or primary productivity, which can be induced, at least in part, by astroclimate changes (Crick et al., 1997; Boullia et al., 2010a). The MS method is popular as it is rapid, non-destructive and reproducible. It offers sufficiently high-resolution acquisitions, which are particularly appropriate for cyclostratigraphic analyses (Mayer and Appel, 1999; Weedon et al., 2004).

The aim of this paper is to contribute to the improvement of the temporal framework of the Early Cretaceous. The interval studied focuses on the Hauterivian/Barremian transition (the *Pseudothurmannia ohmi* and *Taveraidiscus hugii* ammonite zones) outcropping at Río Argos (southeast Spain), the Global boundary Stratotype Section and Point (GSSP) candidate section. The *P. ohmi* Biozone contains an oceanic anoxic event correlated throughout the Western Tethys domain: the Faraoni Oceanic Anoxic Event (F-OAE; Cecca et al., 1994). This event is linked to biological turnovers and to a carbonate productivity crisis (Company et al., 2005; Bodin et al., 2006). The only available durations for these ammonite biozones and the F-OAE are based either on the Pacific magnetostratigraphic model (Ogg and Smith, 2004; Ogg et al., 2008) or on lithological cycle counting (Bodin et al., 2006). Here, we provide a high-resolution cyclostratigraphic analysis from MS measurements. The inferred orbital tuning is independent of magnetostratigraphic models and subjective cycle counting. After comparison of this orbital calibration with previously published data, a new temporal framework is proposed.

## 2. Geological setting

The Río Argos reference section, located in the Subbetic Domain near the town of Caravaca de la Cruz (Fig. 1A), shows a continuous stratigraphic interval for the Hauterivian/Barremian transition (Hoedemaeker and Hergreen, 2003). The deposits are composed of moderately bioturbated, undisturbed marl-limestone couplets. The macrofauna, mainly represented by ammonites and occasionally by brachiopods, irregular echinoids and belemnite guards, is typical of hemipelagic environments, with an estimated water-depth of several hundreds of metres (Hoedemaeker and Leereveld, 1995; Fig. 1B). The abundance of ammonite specimens provides a precise biostratigraphic framework at the subzone level (Company et al.,

2003). The *P. ohmi* Zone extends from bed 144 to bed 171 (Fig. 2), i.e., from the *P. ohmi* first appearance datum (FAD) to the *T. hugii* FAD (Company et al., 2003). The *P. ohmi* zone is divided into the *P. ohmi*, *Pseudothurmannia catulloi* and *Pseudothurmannia picteti* subzones (Fig. 2). Subzones are bounded at the FAD of each index species. The *T. hugii* Zone extends from bed 171 to bed 193, from the *T. hugii* FAD to the *Kotetishvilia nicklesi* FAD. It is divided into the *T. hugii* and *Psilotissotia colombiana* subzones (Fig. 2). Continuous sedimentation is supported by the occurrence of all ammonite subzones and the absence of any evidence of subaerial exposure, erosional features or condensation levels, as revealed by meticulous field observation of sedimentological patterns. An organic-rich horizon, identified in the Late Hauterivian, is associated with the F-OAE (Fig. 2), which constitutes a key level for interbasinal correlations (Baudin, 2005; Bodin et al., 2007).

## 3. Material and methods

### 3.1. Magnetic susceptibility (MS)

A total of 202 rock samples (ca. 10 g) were collected with an even step of 20 cm along a 40.9-m section. Massic MS was measured with a laboratory Kappabridge MFK-1B, Agico®. Empty and sample-filled plastic boxes were measured. Sample values, corrected from blanks, were normalized to sample weight. They are expressed in m<sup>3</sup>/kg and given with a precision of  $\pm 8 \times 10^{-10}$  m<sup>3</sup>/kg (95% confidence level), about two orders of magnitude below the values observed for samples.

### 3.2. Calcium carbonate content

Powdered rock samples were also analysed for calcium carbonate content using a calibrated Bernard calcimeter. Values are given with a precision of between 1 and 5% (Lamas et al., 2005). Data are available from the Pangaea data library: <http://doi.pangaea.de/10.1594/PANGAEA.775274>.

### 3.3. Data processing

The MS series was linearly detrended and then spectral analyses were performed using the multi-taper method (MTM),

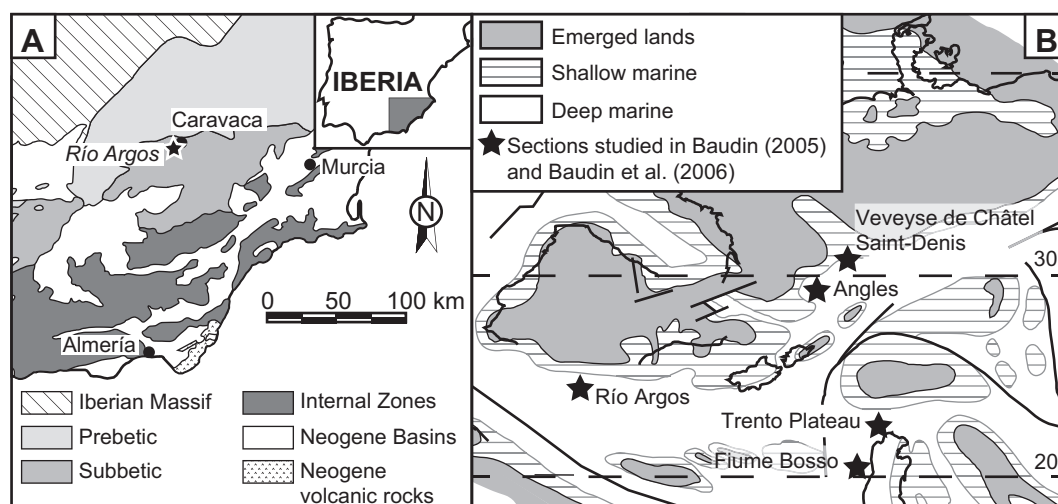


**Fig. 1.** A, simplified geological map of the Betic Cordillera and location of the Río Argos section. B, palaeogeographic map of the Western Tethys for Hauterivian–Barremian times with location of the sections in which the F-OAE is identified. Modified from Baudin (2005).

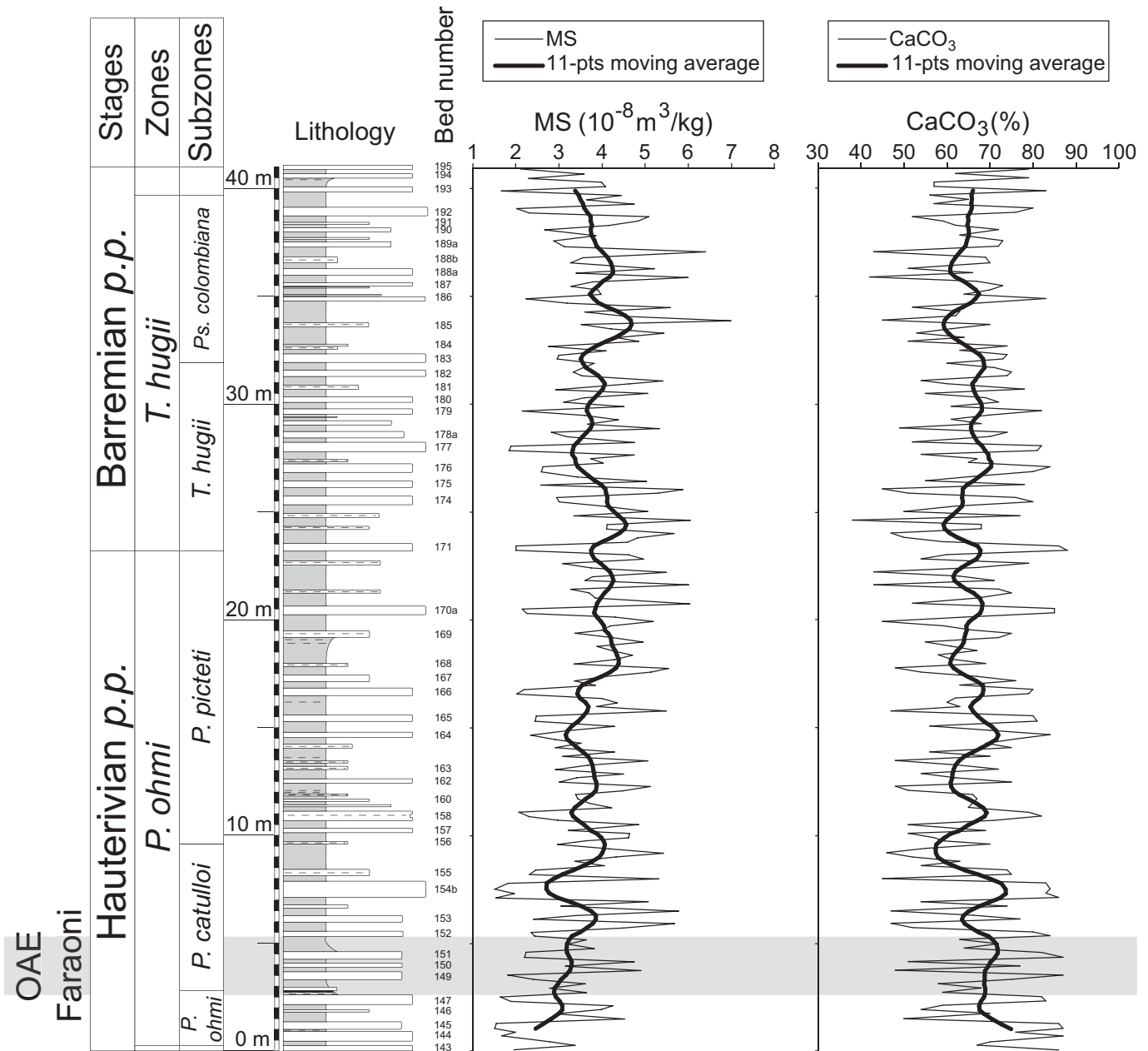


Fig. 2. Magnetic susceptibility (MS) and carbonate content (CaCO<sub>3</sub>) series through the studied interval with an 11-point Gaussian-weighted moving average (thick black line). Lithology: limestone beds are shown in white with the bed numbers indicated alongside, marl interbeds are grey and organic-matter-rich levels are shown in black.

a Fourier-type technique. This popular approach (Maurer et al., 2004; Meyers et al., 2008; Huang et al., 2010) is nonparametric and provides robust power spectral density estimates (Thomson, 1982, 1990). Analyses were carried out with the SSA-MTM toolkit (Ghil et al., 2002), using three  $2\pi$  prolate tapers ( $2\pi$ -MTM) that improve frequency resolution while maintaining suitable confidence levels (e.g., Mann and Park, 1993). The Nyquist frequency (i.e., the highest detectable frequency) is at 2.5 cycles/m (i.e., a period of 0.4 m). Frequency resolution depends on the length of the series. In the case of a  $2\pi$ -MTM analysis, it is defined as  $2/(N \cdot dx)$ , where  $N$  is the number of samples, and  $dx$ , the sample step. With 202 data points, 0.2 m apart, the spectrum frequency resolution  $R$  is here 0.0495 cycle/m. Weedon (2003) recommends interpreting cycles where uncertainty because of frequency

resolution is equal to or less than a factor of two; in other words  $(f_L + R)/(f_L - R) = 2$ , where  $f_L$  is the lowest spectral frequency that can be interpreted. Using 0.0495 cycle/m for  $R$ , the lowest frequency that can be interpreted here with confidence is 0.149 cycle/m (i.e., a period of 6.71 m). Using  $2\pi$ -MTM, at least six repetitions along the studied series are thus required in order to interpret a cycle with confidence.

The significance of observed peaks is tested using a first order autoregressive model, namely AR(1) or red noise, as usually assumed in palaeoclimate series (Mann and Lees, 1996). Justifications for the use of such a red-noise model can be found in Hasselmann (1976) and Frankignoul and Hasselmann (1977). Confidence levels were computed for 90%, 95%, and 99% with the SSA-MTM toolkit (Ghil et al., 2002).

### 3.4. Duration estimates

Using the frequency ratio method (Huang et al., 1993; Boulila et al., 2008), the observed sedimentary cycles were attributed to orbital frequencies, estimated from the astronomical solution of Laskar et al. (2004). Astronomical solutions show that the short eccentricity is the combination of two main periods at 95 and 124 kyr (Laskar et al., 2011). Owing to the chaotic behaviour of the solar system, these periods are not as well constrained as the geochronometer 405-kyr eccentricity for Mesozoic times. A mean period of 100 kyr for the short eccentricity is still identified in most cyclostratigraphic studies (e.g., Park and Herbert, 1987; Olsen and Kent, 1999; Tagliari et al., 2012). Duration estimates using the  $\sim 100$  kyr as reference were successfully applied to Mesozoic series, yielding results in good agreement with those from the reference 405-kyr eccentricity (e.g., Huang et al., 2010). We chose to tune the MS series to the 100-kyr eccentricity period for the following reasons: (1) the stable, well-defined 405-kyr eccentricity geochronometer, recommended to be used for Mesozoic stratigraphic tuning (Laskar et al., 2004), is not well detected, possibly because the interval studied is too short for reliable identification of such cyclicity in spectra; (2) the expression of the 100-kyr eccentricity cycles in the MS series is strong and continuous; (3) although precession cycles are strong and continuous, their periods are not constrained in the Mesozoic because of tidal dissipation effects (Laskar et al., 2004). Taner band-pass filtering was applied to isolate short eccentricity cycles throughout the MS series (Taner, 2000). After filtering, it was then possible to correlate the MS signal to a reference cycle of a constant period of 100 kyr (e.g., Huang et al., 2010) using the AnalySeries “LinAge” function for depth-to-time transformation (Paillard et al., 1996). After reducing sedimentation rate fluctuations by this process, a new  $2\pi$ -MTM analysis produced a less noisy spectrum, which was used to check the reliability of the tuning (Hinnov, 2000). Spectral analyses and tuning were also applied to the calcium carbonate content series, but as these results are close to MS, only the results from the MS series are shown.

## 4. Results

### 4.1. MS and calcium carbonate content

MS values range from  $1.51 \times 10^{-8}$  to  $4.10 \times 10^{-8}$  m<sup>3</sup>/kg in limestone beds and from  $2.78 \times 10^{-8}$  to  $6.99 \times 10^{-8}$  m<sup>3</sup>/kg in marl interbeds (Fig. 2). Calcium carbonate content ranges from 59 to 88% in limestones and from 38 to 79% in marls.

As expected, limestone beds show significantly lower MS values than their adjacent marl interbeds. Calcium carbonate content and MS values display a strong inverse correlation ( $r = -0.94$ ,  $p < 0.001$ ; Fig. 3), indicating that lithology mainly controls the MS variations, as previously reported for pelagic series (Mayer and Appel, 1999; Boulila et al., 2008). An 11-points Gaussian-weighted moving average applied to the series displays this obvious inverse correlation between the two series at lower frequencies.

### 4.2. Spectral analysis

The  $2\pi$ -MTM spectrum of the untuned MS shows peaks above the 95% confidence level (CL) at periods of 3.41 and 0.73 m (Fig. 4A). Peaks at periods of 2.73, 1.02, 0.58 and 0.54 m are above the 90% CL. Using frequency ratio comparisons, sedimentary cycles can be assigned to astronomical periods (Table 1A): (1) the cycles at 3.41 and 2.73 m are associated with the 100-kyr eccentricity (namely “e”); (2) the band centred on 1.02 m is associated with the main

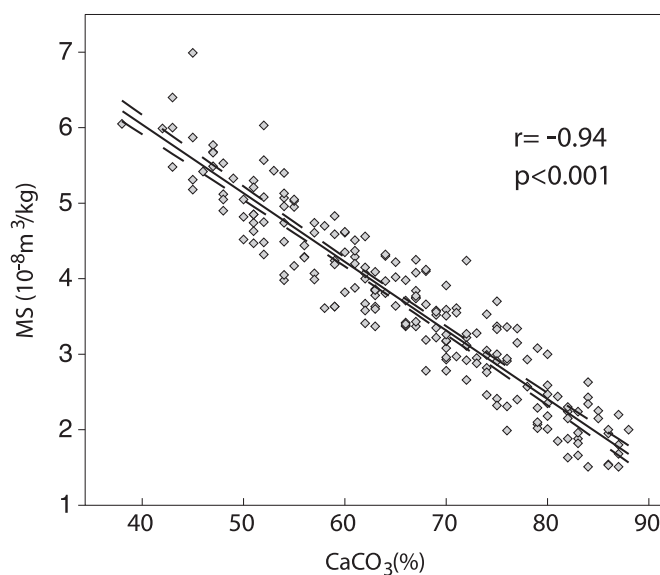


Fig. 3. Magnetic susceptibility (MS) versus calcium carbonate content (CaCO<sub>3</sub>). Full and dashed lines are respectively the best-fit linear fit and the 95% confidence levels of the regression.

obliquity cycle (namely “O1”); and (3) the peaks at 0.73, 0.58 and 0.54 m are associated with the precession cycles (namely “P”).

### 4.3. Duration estimates

The Taner filtering applied to the eccentricity band displays 14 repetitions of the 100-kyr eccentricity cycles on the MS series (Fig. 5C, D). These cycles are in good agreement with the moving averages applied to the series (Fig. 5E). The  $2\pi$ -MTM spectrum of the tuned series (Fig. 4B) shows significant peaks (above 99% CL) at 100 kyr and 21.6 kyr (Fig. 4C). Two peaks appear at 50 kyr and 31.9 kyr, above the 95% CL. A period of  $\sim 700$  kyr is significant at the 95% CL (Fig. 4B); however, the spectral resolution is not good enough to allow this peak to be interpreted (the lower limit for spectrum interpretation is at 0.0043 cycle/kyr or 233 kyr). The minimum duration for the deposit of the series can be calculated as 1.40 myr, with a minimum duration of 0.78 myr for the *P. ohmi* Zone, 0.57 myr for the *T. hugii* Zone and 0.15 myr for the F-OAE (Figs. 5 and 6).

## 5. Discussion

### 5.1. Reliability of the tuning

The untuned spectrum has significant peaks above the 90 and 95% CL, but in the tuned spectrum significant peaks are above the 95 and 99% CL (Fig. 4A, B). Therefore, the tuned spectrum shows a higher signal-to-noise ratio after the tuning procedure has reduced the impact of sedimentation rate variation. As the series was time-constrained at 100 kyr, a corresponding high-power peak is observed on the spectrum at this frequency. Other significant frequencies, which are not constrained, have periods of 50 and 31.9 kyr, close to obliquity periods (46.4 and 36.6 kyr), and a period of 21.8 kyr, close to a precession cycle (21.6 kyr; Fig. 4B, C). The tuned spectrum has, therefore, a higher signal-to-noise ratio and displays peaks at periods close to theoretical orbital periods.

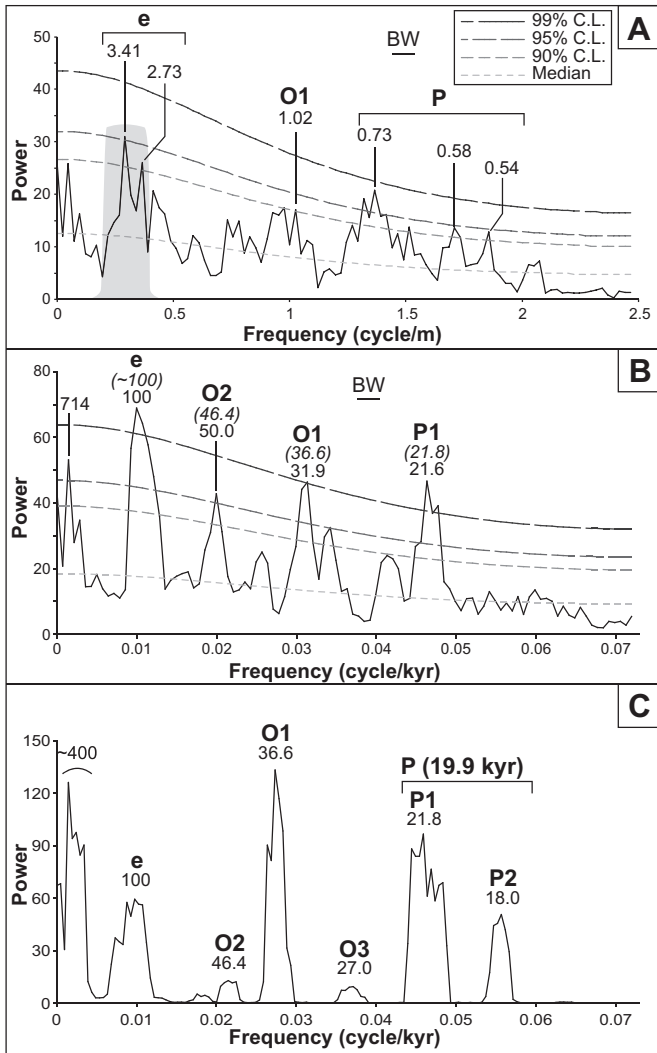


**Fig. 4.**  $2\pi$ -MTM power spectra of magnetic susceptibility (MS) series using the SSA-MTM Toolkit (Ghil et al., 2002). Median represents the red noise modelling smoothed at one-fifth of the Nyquist frequency. 90%, 95% and 99% confidence levels are also shown. The corresponding orbital cycle is indicated in bold. A, spectrum of the untuned MS series. Significant peaks are labelled in metres. Grey-shaded area represents the filtered band of the short (100 kyr) eccentricity cycles used to tune orbitally the MS series. B, spectrum of the 100 kyr-tuned MS series. Significant peaks are labelled in kyr. Cycles above 233 kyr are too long compared to the series length to be correctly identified in the spectrum and are not interpreted (see section 3.3). C, spectrum of the sum of precession (P), obliquity (T), and eccentricity (E) variations in the ETP format (Imbrie et al., 1984), calculated from Laskar et al. (2004) solution over the 129.3–130.7 Ma interval. Peaks are labelled in kyr. Cycles above 233 kyr are too long compared to the series length to be correctly identified in the spectrum and are not interpreted. Comparison of frequency ratios are in Table 1B as follows: e, O1 and P periods correspond to the mean 100-kyr eccentricity, main obliquity and mean precession periods, respectively. Periods of the tuned spectra are then compared to astronomical periods e, O2, O1, O3, P1 and P2.

## 5.2. Comparisons with previous cyclostratigraphic studies

Previous cyclostratigraphic studies of the Hauterivian/Barremian (H/B) boundary were carried out by counting marl/limestone couplets (Bodin et al., 2006) at, in particular, the Angles reference section (Barremian stratotype, Vocontian Basin, southeast France; Figs. 1B and 7). Ammonite successions in the Angles section are well documented (Vermeulen, 2002, 2005). We adapted these data from Angles to the standard zonation proposed by Reboulet et al. (2009) to allow direct comparison with Río Argos. The base of the *T. hugii*

**Table 1A**  
Period ratios between bands identified in the sedimentary spectrum.

	(3.41–2.73 m)	1.02 m	(0.73–0.54 m)
(3.41–2.73 m)	1		
1.02 m	0.337	1	
(0.73–0.54 m)	0.207	0.623	1

**Table 1B**  
Period ratios between orbital cycles deriving from the La2004 solution for the 125–135 Ma interval (Laskar et al., 2004).

	E	O1	P
e	1		
O1	0.364	1	
P	0.204	0.560	1

Zone is defined using the *Taveraidiscus oosteri* FAD, regarded as a synonym of *T. hugii* (Company et al., 2006, 2008). The top of the *T. hugii* Zone corresponds to the *K. nicklesi* FAD (Fig. 7). The base of the *P. ohmi* Zone is defined at the FAD of *P. ohmi*, but different interpretations exist as to the identification of *P. ohmi*, partly because of collection failures (Hoedemaeker et al., 2003). Consequently, at the Angles section, the stratigraphic range of *P. ohmi* does not agree with data from Spain and may have been over-estimated owing to different conceptions of the species (Vermeulen et al., 2002, 2009; Company et al., 2003; Reboulet et al., 2009). Therefore, we chose to compare: (1) the duration of the *T. hugii* Zone, whose boundaries are not problematic; (2) the time interval from the beginning of the F-OAE to the H/B boundary, as these limits are precisely constrained and correlated (Hoedemaeker and Hergreen, 2003; Baudin, 2005); and (3) the durations of the *P. catulloi*, *P. picteti* and *Ps. colombiana* subzones, whose lower boundaries are based on the FAD of the index species, as in Río Argos.

The duration of the time interval from the beginning of the F-OAE to the H/B boundary was estimated as 0.50 myr (Fig. 7; Bodin et al., 2006). This duration is slightly shorter than our estimate (0.71 myr). Using this approach, the duration of the *P. catulloi* Subzone is estimated to be 0.26 myr at both Angles and Río Argos, whereas the *P. picteti* Subzone is estimated at 0.24 myr at Angles but at 0.44 myr for Río Argos. The duration of the *P. catulloi* Subzone at Angles is close to our estimate, but there is a discrepancy between Bodin et al. (2006) and our study as to the duration of the *P. picteti* Subzone. This discrepancy can be explained either by the difficulties met by Bodin et al. (2006) in recognizing all marl-limestone alternations only by field observations or by the presence of a hiatus in the *P. picteti* Subzone. Interestingly, the proposed duration of 0.57 myr for the *T. hugii* Zone is close to the estimate of 0.50 myr by Bodin et al. (2006), although the data are from two different basins (Fig. 7). The duration of the *T. hugii* Subzone is estimated to be 0.36 myr at Angles and 0.30 myr at Río Argos, while for the *Ps. colombiana* Subzone an estimate of 0.14 myr is proposed at Angles compared to 0.27 myr at Río Argos (Fig. 7). These differences can be linked to uncertainties in the position of the base of the *Ps. colombiana* Subzone at Angles, where the index species has only been identified in one bed (Fig. 7).

Using the F-OAE and the *T. hugii* Zone boundaries as reference levels, together with lithological bundles common to the two series, the following correlations are proposed for the 100-kyr cycles (Fig. 7): (1) The e2 cycle is located within the F-OAE. (2) The e3 and e6 cycles are found in carbonate-rich intervals, e3 in the *P. catulloi* Subzone and e6 in the *P. picteti* Subzone. (3) The e7 and e8 cycles are found in the marly interval just below the H/B boundary at Río Argos. This interval is almost completely absent at Angles. (4) The e12 cycle is in the marly interval in the *T. hugii* Zone. This

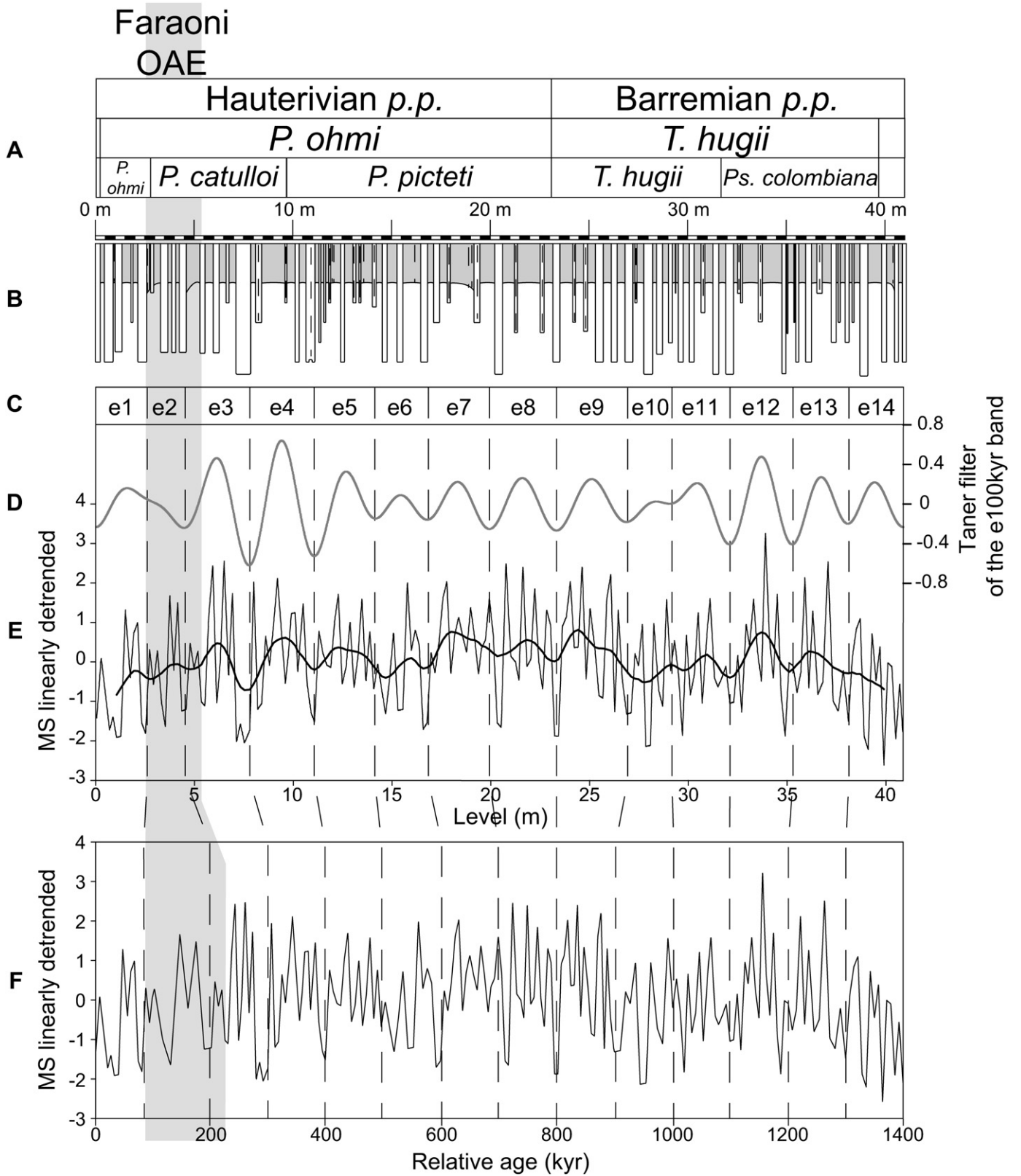


**Fig. 5.** Orbital calibration of the magnetic susceptibility (MS) series. A, standard chronology as explained in Fig. 7; B, lithology; C, interpreted 100-kyr eccentricity cycles from MS minima values; D, Taner filter output of the short eccentricity band performed on the untuned series (cutoff frequencies: 0.195 and 0.399 cycle/m); E, untuned, linearly detrended MS with an 11-point Gaussian-weighted moving average (thick black line); F, 100-kyr-tuned MS.

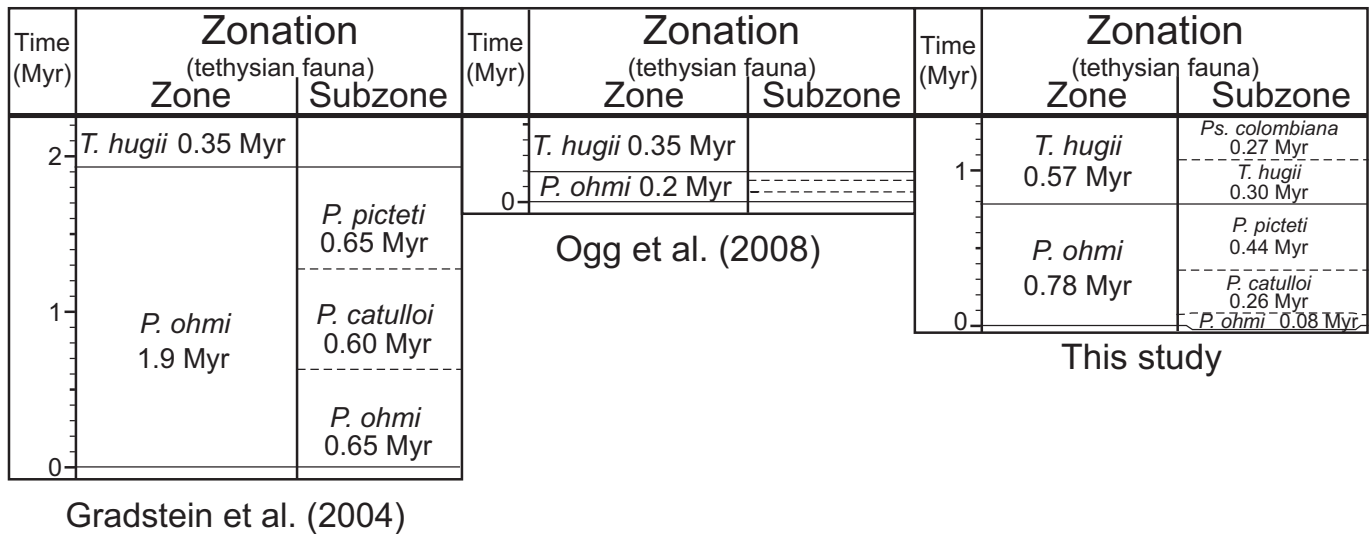


Fig. 6. Durations of ammonite biozones proposed in the GTS 2004 (Gradstein et al., 2004) and Concise GTS 2008 (Ogg et al., 2008) compared with durations proposed in this study.

interval is located at the base of the *Ps. colombiana* Subzone at Río Argos but at the top of the *T. hugii* Subzone (identified by bed counting) at Angles, possibly because of biostratigraphic uncertainties.

The Angles section was probably affected by a short-duration hiatus at the H/B boundary, as suggested by Hoedemaeker and Hergreen (2003). As no such hiatus exists at Río Argos, and as the above correlations tend to confirm the validity of the durations proposed, it is therefore coherent to consider the X.Ag-1 as a GSSP candidate for the H/B boundary.

### 5.3. Comparisons with the GTS

The GTS 2004 (Gradstein et al., 2004) and 2008 (Ogg et al., 2008) report durations for the *P. ohmi* Zone of respectively 1.9 myr and 0.2 myr (Fig. 6), which are markedly different from the 0.78 myr proposed here. The Hauterivian Stage duration is based on the magnetochron model (Ogg and Smith, 2004), while ammonite biozone durations are calculated assuming a fairly linear, increasing trend in Sr-isotope ratio values throughout the Hauterivian (McArthur et al., 2007). The new proposal of the GTS 2008, based on the reassignment of the M10 magnetochron to the Valanginian, suggested by McArthur et al. (2007), considerably reduces the estimated duration for the Hauterivian from 6.4 myr to 3.9 myr. However, in the absence of reliable radiometric dates, current magnetochron durations are based on a constant spreading rate for the Hawaiian crust (Ogg and Smith, 2004). The  $^{87}\text{Sr}/^{86}\text{Sr}$  curve was initially plotted against the stratigraphic levels from the Angles section. To provide durations for ammonite zones, McArthur et al. (2007) proposed an age model that assumes a nearly constant increase in Sr-isotope ratios throughout the Hauterivian, and thus concluded that the Upper Hauterivian section at Angles was affected by higher sedimentation rates. However, field observations of this section show that the marl-limestone alternations for the uppermost Hauterivian–lowermost Barremian are thinner than for the rest of the Hauterivian, thus suggesting lower sedimentation rates. In the absence of reliable radiometric ages, numerical models for magnetochrons and the Sr-isotope ratio curve suffer from uncertainties that explain this observed discrepancy.

Previous cyclostratigraphic studies carried out on Late Jurassic and the Early Cretaceous successions have shown that new

cyclostratigraphic data could improve oceanic spreading models (Sprovieri et al., 2006; Boulila et al., 2010b). An extension of the MS series throughout the Hauterivian could help to provide reliable durations for ammonite biozones within this stage, which should improve duration estimates for magnetochrons and, thus, the precision of the sea-floor spreading model.

### 5.4. Duration of the F-OAE

The Faraoni Level was originally defined as an ammonite-rich level within the Maiolica Formation comprising an interval of alternations between limestone beds and organic-rich black shales (Cecca et al., 1994; Baudin et al., 1999; Fig. 8). This event was coeval with ammonite and calcareous nannoplankton turnovers (Coccioni et al., 1998; Company et al., 2005) and began at the *P. ohmi/P. catulloi* subzone boundary (Fig. 2). Based on a detailed biostratigraphy, organic-rich horizons in Western Tethys basins can be correlated, defining the geographical and temporal extensions of the F-OAE (Baudin et al., 1999; Baudin, 2005; Figs. 1B and 8). According to Baudin (2005) and Baudin et al. (2006), the F-OAE is composed of four to five marl-limestone couplets in the Vocontian Basin and the Subbetic Domain, and seven couplets in the Ultrahelvetec Domain (Switzerland) (Fig. 8). Assuming that a marl-limestone couplet is the expression of precession cycles, Baudin (2005) and Baudin et al. (2006) estimated that the duration of the F-OAE ranged from 80 (Río Argos) to 140 (Ultrahelvetec Domain) kyr. This large range of estimates is probably a result of the difficulty of identifying marl-limestone couplets precisely by field observations alone, when lithology is not well contrasted. High-resolution measurements of carbonate content and MS display 5–6 lithological cycles for the F-OAE interval rather than the 4–5 counted by field observation (Fig. 8). These cycles vary in thickness from 0.40 to 0.63 m. According to power spectra, these values fall within the precession wavelength band (Fig. 4A, B), supporting the hypothesis of Baudin (2005). Therefore, precession cycle counting based on MS and carbonate content measurements lead to a duration of 100–120 kyr for the F-OAE. Short eccentricity-based tuning suggests a duration of 150 kyr for the F-OAE, but tuning such a short event to 100-kyr cycle can lead to significant uncertainties in comparison with the duration of the event. We therefore propose a duration range for the F-OAE of 100–150 kyr.

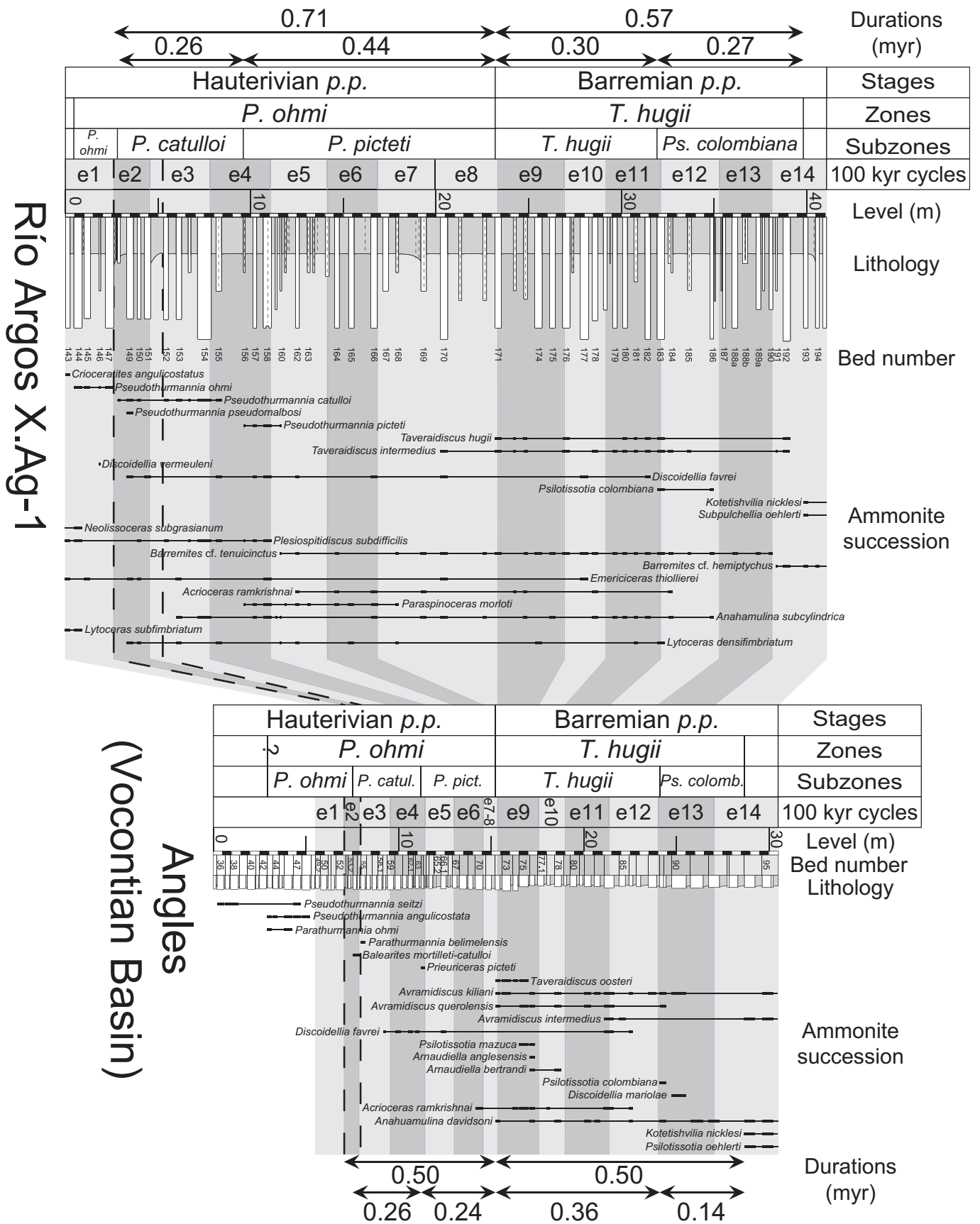


**Fig. 7.** Correlation and comparative lithology, biostratigraphy and durations for the Río Argos X.Ag-1 and Angles sections. Río Argos X.Ag-1: bed numbers, ammonite succession and biozonation are from Company et al. (2003, 2005). Angles: bed numbers and lithology are from Vermeulen (2002). Ammonite succession is from Vermeulen (2005). Durations are from Bodin et al. (2006). Standard biozonation is adapted from data in Vermeulen (2005). Note the uncertainty of the lower boundary of the *P. ohmi* Zone owing to different conceptions of the index species. The 100-kyr cycles are projected from those identified at Río Argos in this study.

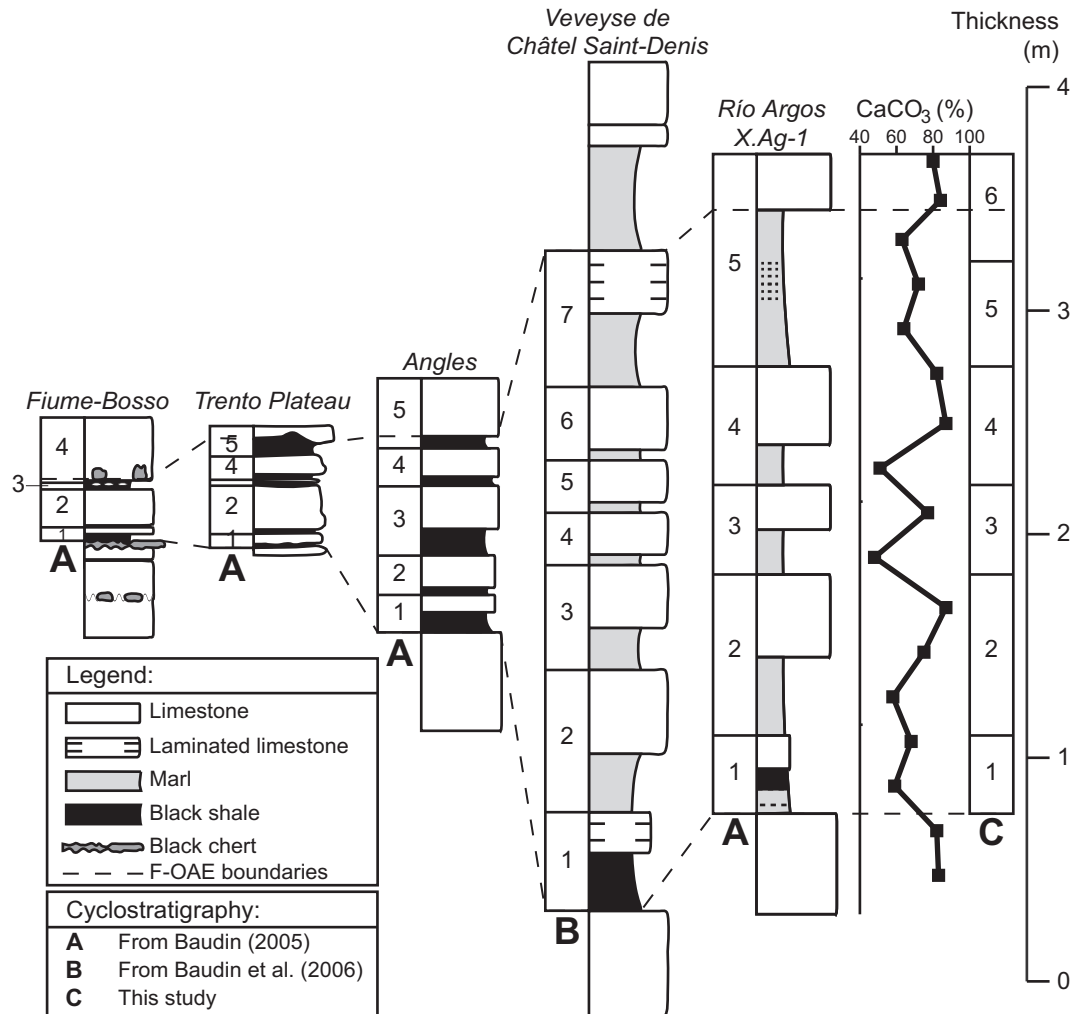


**Fig. 8.** Correlations of the F-OAE between different sections from the Western Tethys and Río Argos X.Ag-1. Precession-cycle counts are also shown for each section. For the Río Argos section, cycle counts are based (A) on field observation (Baudin, 2005) and (C) on CaCO<sub>3</sub> content fluctuations (this study). Scale thickness is identical for all sections.

## 6. Conclusions

The MS measurements for the Hauterivian–Barremian transition at the reference Río Argos section exhibit a cyclic pattern that is attributable to Earth's orbital parameters. An orbital tuning based on the 100-kyr eccentricity is proposed to improve the time-frame of this period. The duration of the *P. ohmi* Biozone is estimated at 0.78 myr, that of the *T. hugii* Biozone at 0.57 myr, and that of the Faraoni Oceanic Anoxic Event at 100–150 kyr. These durations are in the same range as those previously reported in cyclostratigraphic analyses carried out on the Angles section. Correlations between the two sections tend to show that a short-duration hiatus probably affected the Angles section, confirming the Río Argos section as a valid candidate for GSSP. Our proposed durations may be useful for improving the Geologic Time Scale 2008, in which stage and biozone durations are largely dependent on magnetostratigraphic and Sr-isotope trend models. The biozone durations reported here, together with further studies on the entire Hauterivian Stage, should help to improve the accuracy of the next geologic time scale.

## Acknowledgements

Funding for this research was provided by the ANR project "Astronomical Time Scale for the Mesozoic and Cenozoic eras". We

are grateful to Rémi Laffont (CNRS research engineer, UMR/CNRS 6282 Biogeosciences) for help with Matlab and Carmela Chateau-Smith (University of Burgundy) for help with our English. We acknowledge the two anonymous reviewers for their constructive advice.

## References

- Baudin, F., 2005. A Late Hauterivian short-lived anoxic event in the Mediterranean Tethys: the 'Faraoni Event'. *Comptes Rendus Geoscience* 337, 1532–1540.
- Baudin, F., Bulot, L.G., Cecca, F., Coccioni, R., Gardin, S., Renard, M., 1999. An equivalent of the "Faraoni Level" in the South-East of France, possible evidence for a late Hauterivian anoxic event in the Mediterranean Tethys. *Bulletin de la Société Géologique de France* 170, 487–498.
- Baudin, F., Busnardo, R., Beltran, C., de Rafélis, M., Renard, M., Charollais, J., Clavel, B., 2006. Enregistrement de l'événement anoxique Faraoni (Hauterivien supérieur) dans le domaine ultrahelvétique. *Revue de Paléobiologie* 25, 525–535.
- Bodin, S., Godet, A., Föllmi, K.B., Vermeulen, J., Arnaud, H., Strasser, A., Fiet, N., Adatte, T., 2006. The late Hauterivian Faraoni oceanic anoxic event in the western Tethys: evidence from phosphorus burial rates. *Palaeogeography, Palaeoclimatology, Palaeoecology* 235, 245–264.
- Bodin, S., Godet, A., Matera, V., Steinmann, P., Vermeulen, J., Gardin, S., Adatte, T., Coccioni, R., Föllmi, K.B., 2007. Enrichment of redox-sensitive trace metals (U, V, Mo, As) associated with the late Hauterivian Faraoni oceanic anoxic event. *International Journal of Earth Sciences* 96, 327–341.
- Boullia, S., de Rafélis, M., Hinnov, L.A., Gardin, S., Galbrun, B., Collin, P.Y., 2010a. Orbitally forced climate and sea-level changes in the Paleocene Tethyan domain (marl-limestone alternations, Lower Kimmeridgian, SE France). *Palaeogeography, Palaeoclimatology, Palaeoecology* 292, 57–70.

- Boullia, S., Galbrun, B., Hinnov, L.A., Collin, P.Y., 2008. High-resolution cyclostratigraphic analysis from magnetic susceptibility in a Lower Kimmeridgian (Upper Jurassic) marl-limestone succession (La Méouge, Vocontian Basin, France). *Sedimentary Geology* 203, 54–63.
- Boullia, S., Galbrun, B., Hinnov, L.A., Collin, P.Y., Ogg, J.G., Fortwengler, D., Marchand, D., 2010b. Milankovitch and sub-Milankovitch forcing of the Oxfordian (Late Jurassic) Terres Noires Formation (SE France) and global implications. *Basin Research* 22, 717–732.
- Cecca, F., Marini, A., Pallini, G., Baudin, F., Bégouen, V., 1994. A guide level of the uppermost Hauterivian (Lower Cretaceous) in the pelagic succession of Umbria-Marche Apennines (Central Italy): the Faraoni Level. *Rivista Italiana di Paleontologia e Stratigrafia* 99, 551–568.
- Coccioni, R., Baudin, F., Cecca, F., Chiari, M., Galeotti, S., Gardin, S., Salvini, G., 1998. Integrated stratigraphic, palaeontological, and geochemical analysis of the uppermost Hauterivian Faraoni Level in the Fiume-Bosso section, Umbria-Marche Apennines, Italy. *Cretaceous Research* 19, 1–23.
- Company, M., Aguado, R., Sandoval, J., Tavera, J.M., de Cisneros, C.J., Vera, J.A., 2005. Biotic changes linked to a minor anoxic event (Faraoni Level, latest Hauterivian, early Cretaceous). *Palaeogeography, Palaeoclimatology, Palaeoecology* 224, 186–199.
- Company, M., Fözy, I., Sandoval, J., Tavera, J.M., 2006. *Deitanites* n.g. and other related ammonites. Their significance within the family Holcodiscidae (Lower Cretaceous, Mediterranean region). *Neues Jahrbuch für Geologie und Paläontologie, Monatshefte* 2006, 1–14.
- Company, M., Sandoval, J., Tavera, J.M., 2003. Ammonite biostratigraphy of the uppermost Hauterivian in the Betic Cordillera (SE Spain). *Geobios* 36, 685–694.
- Company, M., Sandoval, J., Tavera, J.M., Aoutem, M., Ettachfni, M., 2008. Barremian ammonite faunas from the western High Atlas, Morocco – biostratigraphy and palaeobiogeography. *Cretaceous Research* 29, 9–26.
- Crick, R.E., Ellwood, B.B., El Hassani, A., Feist, R., Hladil, J., 1997. Magneto-susceptibility event and cyclostratigraphy (MSEC) of the Eifelian–Givetian GSSP and associated boundary sequences in North Africa and Europe. *Episodes* 20, 167–175.
- Ellwood, B.B., Crick, R.E., El Hassani, A., Benoist, S.L., Young, R.H., 2000. Magneto-susceptibility event and cyclostratigraphy method applied to marine rocks: detrital input versus carbonate productivity. *Geology* 28, 1135–1138.
- Frankignoul, C., Hasselmann, K., 1977. Stochastic climate models. 2. Application to sea-surface temperature anomalies and thermocline variability. *Tellus* 29, 289–305.
- Ghil, M., Allen, M.R., Dettinger, M.D., Ide, K., Kondrashov, D., Mann, M.E., Robertson, A.W., Saunders, A., Tian, Y., Varadi, F., Yiou, P., 2002. Advanced spectral methods for climatic time series. *Reviews of Geophysics* 40, 3.1–3.41.
- Gradstein, F.M., Ogg, J.G., Smith, A.G., 2004. *A Geologic Time Scale 2004*. Cambridge University Press, Cambridge, 610 pp.
- Hasselmann, K., 1976. Stochastic climate models. 1. Theory. *Tellus* 28, 473–485.
- Hays, J.D., Imbrie, J., Shackleton, N.J., 1976. Variations in Earth's orbit – pacemaker of ice ages. *Science* 194, 1121–1132.
- Hinnov, L.A., 2000. New perspectives on orbitally forced stratigraphy. *Annual Review of Earth and Planetary Sciences* 28, 419–475.
- Hinnov, L.A., Ogg, J.G., 2007. Cyclostratigraphy and the astronomical time scale. *Stratigraphy* 4, 239–251.
- Hoedemaeker, P.J., Hergreen, G.F.W., 2003. Correlation of Tethyan and Boreal Berriasian–Barremian strata with emphasis on strata in the subsurface of the Netherlands. *Cretaceous Research* 24, 253–275.
- Hoedemaeker, P.J., Leereveld, H., 1995. Biostratigraphy and sequence stratigraphy of the Berriasian–Lowest Aptian (Lower Cretaceous) of the Rio Argos succession, Caravaca, SE Spain. *Cretaceous Research* 16, 195–230.
- Hoedemaeker, P.J., Reboulet, S., Aguirre-Urreta, M.B., Alsen, P., Aoutem, M., Atrops, F., Barragán, R., Company, M., González Arreola, C., Klein, J., Lukeneder, A., Ploch, I., Raisossadat, N., Rawson, P.F., Ropolo, P., Vašíček, Z., Vermeulen, J., Wippich, M.G.E., 2003. Report on the 1st International Workshop of the IUGS Lower Cretaceous Ammonite Working Group, the 'Kilian Group' (Lyon, 11 July 2002). *Cretaceous Research* 24, 89–94.
- Huang, C.J., Hesselbo, S.P., Hinnov, L., 2010. Astrochronology of the late Jurassic Kimmeridge Clay (Dorset, England) and implications for Earth system processes. *Earth and Planetary Science Letters* 289, 242–255.
- Huang, Z., Ogg, J.G., Gradstein, F.M., 1993. A quantitative study of Lower Cretaceous cyclic sequences from the Atlantic Ocean and the Vocontian Basin (SE France). *Paleoceanography* 8, 275–291.
- Husson, D., Galbrun, B., Laskar, J., Hinnov, L.A., Thibault, N., Gardin, S., Locklair, R.E., 2011. Astronomical calibration of the Maastrichtian (Late Cretaceous). *Earth and Planetary Science Letters* 305, 328–340.
- Imbrie, J., Hays, J.D., Martinson, D.G., McIntyre, A., Mix, A.C., Morley, J.J., Pisias, N.G., Prell, W.L., Shackleton, N.J., 1984. The orbital theory of Pleistocene climate: support from a revised chronology of the marine  $\delta^{18}\text{O}$  record. In: Berger, A., Imbrie, J., Hays, J., Kukla, G., Saltzman, B. (Eds.), *Milankovitch and Climate: Understanding the Response to Astronomical Forcing*. D. Reidel Publishing Company, Dordrecht, pp. 269–303.
- Lamas, F., Irigaray, C., Oteo, C., Chacon, J., 2005. Selection of the most appropriate method to determine the carbonate content for engineering purposes with particular regard to marls. *Engineering Geology* 81, 32–41.
- Laskar, J., Fienga, A., Gastineau, M., Manche, H., 2011. La2010: a new orbital solution for the long-term motion of the Earth. *Astronomy & Astrophysics* 532, A89.
- Laskar, J., Robutel, P., Joutel, F., Gastineau, M., Correia, A.C.M., Levrard, B., 2004. A long-term numerical solution for the insolation quantities of the Earth. *Astronomy & Astrophysics* 428, 261–285.
- Locklair, R.E., Sageman, B.B., 2008. Cyclostratigraphy of the Upper Cretaceous Niobrara Formation, Western Interior, USA: a Coniacian–Santonian orbital time-scale. *Earth and Planetary Science Letters* 269, 539–552.
- Lourens, L.J., Hilgen, F.J., Shackleton, N.J., Laskar, J., Wilson, D., 2004. The Neogene Period. In: Gradstein, F.M., Ogg, J.G., Smith, A.G. (Eds.), *A Geologic Time Scale 2004*. Cambridge University Press, Cambridge, pp. 409–440.
- Mann, M.E., Lees, J.M., 1996. Robust estimation of background noise and signal detection in climatic time series. *Climatic Change* 33, 409–445.
- Mann, M.E., Park, J., 1993. Spatial correlations of interdecadal variation in global surface temperatures. *Geophysical Research Letters* 20, 1055–1058.
- Maurer, F., Hinnov, L.A., Schlager, W., 2004. Statistical time series analysis and sedimentological tuning of bedding rhythms in a Triassic basinal succession (Southern Alps, Italy). In: d'Argenio, B., Fischer, A.G., Premoli Silva, I., Weissert, H., Ferreri, V. (Eds.), 2004. *Cyclostratigraphy: Approaches and Case Histories*. SEPM Special Publication 81, pp. 83–99.
- Mayer, H., Appel, E., 1999. Milankovitch cyclicity and rock-magnetic signatures of palaeoclimatic change in the Early Cretaceous Biancone Formation of the Southern Alps, Italy. *Cretaceous Research* 20, 189–214.
- McArthur, J.M., Janssen, N.M.M., Reboulet, S., Leng, M.J., Thirlwall, M.F., van de Schootbrugge, B., 2007. Palaeotemperatures, polar ice-volume, and isotope stratigraphy (Mg/Ca, delta O-18, delta C-13, Sr-87/Sr-86): the Early Cretaceous (Berriasian, Valanginian, Hauterivian). *Palaeogeography, Palaeoclimatology, Palaeoecology* 248, 391–430.
- Meyers, S.R., Sageman, B.B., Pagani, M., 2008. Resolving Milankovitch: consideration of signal and noise. *American Journal of Science* 308, 770–786.
- Ogg, J.G., Ogg, G., Gradstein, F.M., 2008. *The Concise Geologic Time Scale*. Cambridge University Press, Cambridge, 184 pp.
- Ogg, J.G., Smith, A.G., 2004. The geomagnetic polarity time scale. In: Gradstein, F.M., Ogg, J.G., Smith, A.G. (Eds.), *A Geologic Time Scale 2004*. Cambridge University Press, Cambridge, pp. 63–86.
- Olsen, P.E., Kent, D.V., 1999. Long-period Milankovitch cycles from the Late Triassic and Early Jurassic of eastern North America and their implications for the calibration of the Early Mesozoic time-scale and the long-term behaviour of the planets. *Philosophical Transactions of the Royal Society A, Mathematical, Physical and Engineering Sciences* 357, 1761–1786.
- Paillard, D., Labeyrie, L., Yiou, P., 1996. Macintosh program performs time-series analysis. *Eos, Transactions American Geophysical Union* 77, 379.
- Park, J., Herbert, T.D., 1987. Hunting for paleoclimatic periodicities in a geologic time-series with an uncertain time scale. *Journal of Geophysical Research* 92, 14027–14040.
- Reboulet, S., Klein, J., Barragán, R., Company, M., González-Arreola, C., Lukeneder, A., Raisossadat, S.N., Sandoval, J., Szives, O., Tavera, J.M., Vašíček, Z., Vermulen, J., 2009. Report on the 3rd International Meeting of the IUGS Lower Cretaceous Ammonite Working Group, the 'Kilian Group' (Vienna, Austria, 15th April 2008). *Cretaceous Research* 30, 496–502.
- Reynolds, R.L., King, J.W., 1995. Magnetic records of climate-change. *Reviews of Geophysics* 33, 101–110.
- Sprovieri, M., Coccioni, R., Lirer, F., Pelosi, N., Lozar, F., 2006. Orbital tuning of a Lower Cretaceous composite record (Maiolica Formation, central Italy). *Paleoceanography* 21, PA4212.
- Tagliari, C.V., Scarparo Cunha, A.A., Gomes Paim, P.S., 2012. Orbital-driven cyclicity and the role of halokinesis on accommodation within siliciclastic to carbonate, shallow-water Albian deposits in the Espírito Santo Basin, southeastern Brazil. *Cretaceous Research*. doi:10.1016/j.cretres.2011.11.008.
- Taner, M.T., 2000. *Attributes Revisited*. Technical Publication, Rock Solid Images, Inc, Houston, Texas. URL: [http://www.rocksolidimages.com/pdf/attrib\\_revisited.htm](http://www.rocksolidimages.com/pdf/attrib_revisited.htm).
- Thomson, D.J., 1982. Spectrum estimation and harmonic-analysis. *Proceedings of the IEEE* 70, 1055–1096.
- Thomson, D.J., 1990. Quadratic-inverse spectrum estimates – applications to paleoclimatology. *Philosophical Transactions of the Royal Society of London Series A – Mathematical, Physical and Engineering Sciences* 332, 539–597.
- Vermeulen, J., 2002. Étude stratigraphique et paléontologique de la famille des Pulchelliidae (Ammonoidea, Ammonitina, Endemocerataceae). *Géologie Alpine, Mémoire Hors Série* 42, 333 pp.
- Vermeulen, J., 2005. Boundaries, ammonite fauna and main subdivisions of the stratotype of the Barremian. *Géologie Alpine, Série Spéciale "Colloques et excursions"* 7, 147–173.
- Vermeulen, J., Bert, D., Autran, G., 2002. Éléments pour la biostratigraphie ammonitique de l'Hauterivien terminal méditerranéen. *Riviera Scientifique* 86, 71–87.
- Vermeulen, J., Duyé, J.P., Lazarin, P., Leroy, L., Mascarelli, E., 2009. Nouvelles données taxinomiques sur la famille des Crioceratitidae Gill, 1871 (Ancyloceratina, Ancyloceratoidea). *Riviera Scientifique* 92, 65–76.
- Voigt, S., Schönfeld, J., 2010. Cyclostratigraphy of the reference section for the Cretaceous white chalk of northern Germany, Lagerdorf-Kronsmoor: aq late Campanian–early Maastrichtian orbital time scale. *Palaeogeography, Palaeoclimatology, Palaeoecology* 287, 67–80.
- Weedon, G.P., 2003. *Time-Series Analysis and Cyclostratigraphy*. Cambridge University Press, Cambridge, 274 pp.
- Weedon, G.P., Coe, A.L., Gallois, R.W., 2004. Cyclostratigraphy, orbital tuning and inferred productivity for the type Kimmeridge Clay (Late Jurassic), southern England. *Journal of the Geological Society, London* 161, 655–666.